Research Square

Preprints are preliminary reports that have not undergone peer review.
They should not be considered conclusive, used to inform clinical practice,
or referenced by the media as validated information.

Effects of HIF-1α Knockdown on Cell Viability and Oxidative Stress in Oxygen–Glucose-Deprived Human Brain Microvascular Endothelial Cells

Min Wang
Dali University
Yabin Shen
Nantong University
Huaqiu Chen
Xichang University
Guangming Wang
wgm1991@dali.edu.cn

Dali University

Research Article

Keywords: Ischemic stroke, HIF-1α, Brain microvascular endothelial cells, Oxygen–glucose deprivation, Oxidative stress, HIF1A-AS2

Posted Date: November 11th, 2026

DOI: https://doi.org/10.21203/rs.3.rs-11497081/v1

License: This work is licensed under a Creative Commons Attribution 4.0 International License.
Read Full License

Additional Declarations: No competing interests reported.

Abstract

Hypoxia-inducible factor-1α (HIF-1α) is a key regulator of cellular responses to hypoxia. This study examined the effects of HIF-1α knockdown on cell viability and oxidative stress in human brain microvascular endothelial cells and explored a putative HIF1A-AS2/miR-27a-3p/HIF1A regulatory relationship. Public stroke-related transcriptomic datasets were analyzed, and hCMEC/D3 cells were subjected to oxygen–glucose deprivation (OGD). Lentiviral HIF-1α knockdown was assessed by reverse transcription–quantitative PCR (RT-qPCR) and western blotting. Cell Counting Kit-8 (CCK-8) signals, reactive oxygen species (ROS), and malondialdehyde (MDA) were measured. Protein interaction and enrichment analyses were combined with regulatory-network prediction and dual-luciferase reporter assays. HIF1A expression was elevated in the analyzed stroke-related datasets, and OGD increased HIF-1α expression in hCMEC/D3 cells. HIF-1α knockdown increased CCK-8 signals under OGD; however, MDA levels were higher in the shHIF-1α + OGD group than in the Control + OGD group. OGD increased ROS levels in both control and HIF-1α-knockdown cells. Reporter assays supported sequence-dependent interactions of miR-27a-3p with HIF1A-AS2 and HIF1A reporter constructs. These findings indicate that increased CCK-8 signals following HIF-1α knockdown coexist with increased MDA under OGD, rather than demonstrating uniform protection against oxidative injury. The reporter results suggest a potential regulatory relationship, but its contribution to the cellular phenotype requires functional rescue experiments. The divergent endpoints also warrant independent assessment of cell survival and lipid peroxidation before a protective role is assigned to HIF-1α knockdown.

1. Introduction

Globally, stroke is the second leading cause of death and the third leading cause of morbidity and mortality [1]. The economic systematic review of IS shows that the global average annual expenditure per IS patient is $27,702, while the lifetime average expenditure is $67,900 [2]. They are roughly divided into ischemic stroke and hemorrhagic stroke according to the type of injury (vascular occlusion or rupture). During the pathogenesis of stroke, the body activates complex molecular and cellular mechanisms through cascade reactions [3, 4].

Hypoxia-inducible factor-1 (HIF-1) is one of the important regulatory proteins expressed in cells after hypoxia, which controls the expression of more than 700 target genes that mediate adaptive and pathological processes, which have been found to be involved in the pathophysiology of many neurological diseases, especially IS [5]. HIF1 is a heterodimer consisting of one β subunit (HIF-1β, also called ARNT) and one of three α subunits (HIF-1α, HIF-2α, or HIF-3α) [6]. HIF-1β exists stably in the cytoplasm or nucleus and plays a structural role; HIF-1α exists in the cytoplasm and is the active subunit of HIF1, which is a key molecule in response to hypoxic stress. Under the trigger of oxygen homeostasis imbalance, HIF-1α achieves nuclear translocation through dynamic regulation of ubiquitination-deubiquitination, and forms a heterodimeric complex with structurally expressed HIF-1β. The transcription factor accurately recognizes the hypoxia response element (HRE) on the target genomic DNA through its basic helix-loop-helix domain, cooperates with histone-modifying enzymes and co-

activators, constructs a multi-dimensional gene expression regulatory network, and finally realizes a spatiotemporal-specific regulatory program for angiogenesis, glycolysis and cell survival. Hypoxia is the most important physiological regulator of HIF-1α expression. Under normal oxygen saturation, the expression of HIF-1α is basically undetectable. HIF-1α stably exists in the cytoplasm when oxygen concentration decreases [7]. Therefore, it is of practical value to explore the expression changes of HIF-1α in ischemic stroke and the related mechanism of regulating HIF-1α expression in how to improve the prognosis of ischemic stroke.

lncRNA has the function of regulating the expression of target genes after binding to miRNA. Studies have shown that: A regulatory network can be formed among lncRNA, miRNA and mRNA, namely: lncRNA-miRNA-mRNA, specifically, lncRNA is adsorbed onto miRNA to regulate miRNA expression, and then miRNA binds to the promoter region of mRNA to affect mRNA expression [8]. The results of clinical studies in patients with ischemic stroke show that the content of lncHIF1A-AS2 in peripheral blood of patients with ischemic stroke increases, which leads to the increase of HIF-1α expression; After effective treatment, the content of lncHIF1A-AS2 decreases, which leads to the decrease of HIF-1α expression, thus promoting angiogenesis and obtaining a better prognosis [9]. There is a regulatory effect between lncRNA and mRNA [10, 11]. There may be miRNA between lncHIF1A-AS2 and HIF-1α as an intermediate molecular substance involved or mediated the regulation of HIF-1α expression by lncHIF1A-AS2.

miRNA is a kind of endogenous short-stranded non-coding RNA with a sequence of about 19–25 nucleotides in length. It binds to target genes for post-transcriptional regulation and plays a role in gene silencing or inhibiting translation. Our previous studies have found that five miRNAs, including miR-27a-3p, can be used as molecular markers for diagnosis and molecular targets for treatment of ischemic cerebral infarction [12]. The miR-27 family includes miR-27a and miR-27b, and miR-27a in turn includes miR-27a-3p and miR-27a-5p, both located on human chromosome 17. They are involved in tumorigenesis, cell proliferation, apoptosis, invasion, metastasis and angiogenesis, and are molecular markers and potential therapeutic targets of tumors [13]. In the study of cultured cerebral microvascular endothelial cells, miR-27a-3p has been found to interact with related signaling pathways to mediate cerebral vascular integrity and repair [14]. The abnormal expression of miR-27a-3p in peripheral blood of stroke patients can aggravate brain tissue damage and neuroinflammation, thus increasing the area of necrosis [15]. In rat MCAO model and cell experimental studies, miR-27a-3p was found to be involved in ischemia-hypoxia injury through inflammatory response and apoptosis [16]. In vivo and in vitro studies have shown that miR-27a-3p is involved in the maintenance of blood brain barrier (BBB) permeability [17, 18]. Bioinformation analysis showed that miR-27a-3p is one of the target miRNAs regulated by lncHIF1A-AS2 [10, 11]. All the above studies have shown that the lncRNA-miRNA-mRNA pathway is involved in various physiological or pathophysiological conditions, so the lncRNA-miRNA-mRNA pathway may also exist in ischemic cerebral infarction.

Therefore, the purpose of this study is to explore the expression changes of HIF-1α in ischemic stroke and the related mechanism of regulating HIF-1α expression, which has certain practical value in how to improve the prognosis of ischemic stroke.

2. Materials and Methods

2.1 Data acquisition and processing of gene expression

A search was performed in the NCBI's Gene Expression Omnibus (GEO) database (https://www.ncbi.nlm.nih.gov/geo/) using the keywords "ischemic stroke" and "Homo sapiens" or "MCAO" and “Rattus norvegicus”, after screening, GSE16561, GSE58294, and GSE22255 were used as training data sets. The datasets are listed in Table 1. Pooling the datasets within each group and principal component analysis of the pooled training datasets utilizing the "ggplot2" package in R (version 4.2.1) (principal component analysis, PCA); consistency was ensured and any potential bias was eliminated, and the expression of HIF-1α in the ischemic stroke and control groups was verified using the Wilcoxon rank sum test in R.

Table 1
GEO dataset information

GEO accession	Platform	Country	Year	Healthy controls (n)	Stroke patients (n)
GSE16561	GPL6883	USA	2010	24	39
GSE58294	GPL570	USA	2014	23	69
GSE22255	GPL570	Portugal	2011	20	20
GSE37587	GPL6883	USA	2015	0	34
GSE25414	GPL570	Spain	2010	12	0
GSE119121	GPL6247	Belgium	2018	7	40
Note: only GSE16561, GSE58294 and GSE22255 were used as training datasets in the present study					

2.2 Group difference analysis and co-expression analysis

Differentially expressed genes between the ischemic stroke group and the normal control in the training group were detected using the R package "limma" of BiocManager. The filter criteria were set to adjusted $p < 0.05$ and log fold change (FC) > 0.58. The heatmap was created using the R software "heatmap" package, and the samples in the training set were divided into high and low expression groups, and the results were visualized. Co-expression analysis of related genes was performed using the "corrplot" package.

2.3 Construction of HIF-1α-related protein interaction and functional enrichment analysis

The PPI network of HIF-1α-related proteins was established in the STRING database (https://cn.string116db.org/). Gene Ontology (GO) and Kyoto encyclopedia of genes and genomes (KEGG) enrichment analyses were performed on genes associated with HIF-1α using R (4.2. 1) version "ggplot2" package and the results were visualized.

2.4 Cell culture and construction of OGD model

Human cerebrovascular endothelial cell line (hCMEC/D3) was purchased from Hunan Fenghui Biotechnology (Hunan, China), cells were cultured in RPMI-1640 basal medium containing 10% fetal bovine serum, 100 U/ml penicillin, 100 μg/ml streptomycin, and 2 mM L-glutamine. The incubation process was carried out in 5% CO_2, 37 ℃ constant temperature humidification incubator. The cells were placed in 1% FBS medium, cultured for 12h according to the above conditions, and then the cells in the logarithmic growth phase were taken for OGD modeling. Modeling conditions were placed in sugar-free low serum (1%FBS) medium, OGD injury was induced by incubation in a humidified incubator exposed to 37°C under hypoxic conditions (92% N2, 5% CO2, 3% O2) for 2 h. Cells cultured under conventional culture conditions were used as blank Control group (Control).

2.5 Cell transfection

The hCMEC/D3 cells in the logarithmic growth phase were seeded into 12-well plates according to 1 × 10^5 cells per well, and the cell adherence and growth were observed 24h later. When the degree of cell confluence reaches about 50%, knockdown HIF-1α lentivirus infection can be performed. The lentivirus (mdl company) was removed from the refrigerator at − 80°C and melted on ice. The original medium was aspirated and the volume of virus was calculated based on 100 PFU per cell, Add 1ml of complete medium, corresponding virus volume and 1μl of Polybrene, mix well and transfer to incubator for culture, after 24 hours, the virus solution was aspirated, and then complete culture medium was added to continue culture for 24 hours. Add proper amount of puromycin to screen until there is no obvious cell death. Observe the fluorescence effect, take photos and record the experimental results.

2.6 Real-time fluorescence quantitative PCR (RT-qPCR)

When the cell growth reaches more than 85%, the original culture medium in the six-well plate is aspirated. Washing was performed once with PBS buffer and 800 μl TRIzol was added per well, Let stand at room temperature for 5 minutes. Use a 200μl pipette to gently pipet along the well wall at multiple angles (to avoid bubbles), After the solution is homogeneous, the lysate is transferred to a 1.5 ml RNase-free EP tube of. 160μl chloroform per 800μl TRIzol as per kit manual. RNA concentration was determined using an ultramicro ultraviolet spectrophotometer. RNase-free centrifuge tube is used to configure the reverse transcription reaction system mixture and add it to the centrifuge tube 5 × SweScript All-in-One SuperMix for qPCR 2 μl, gDNA Remover 0.5 μl, Total RNA 0.1 ng-5 μg/10 pg-0. 5 μg (x), Nuclease-Free Water (10-2.5-x) μl, Total volume 10 μl. After thoroughly mixing, heat at 25°C for 5 minutes, 42°C for 30 minutes, and 85°C for 5 seconds, then add 140 μl of DEPC water and mix well for later use.

The RT-qPCR reaction system was configured in the qPCR test tube: 4 μl of template, 10 μl of 2 × SYBR Green qPCR Master Mix, 1 μl of upstream primer and downstream primer, 5 μl of deionized water, and 20 μl of total reaction system. Samples were loaded in groups, and the experiment was started using a qPCR instrument: (a) the temperature was 95°C, and the pre-denaturation was performed for 1 min (one cycle); (b) Temperature 95°C, denaturation for 10 seconds (40 cycles); (c) The temperature is 60°C,

annealing for 30 seconds (40 cycles), and fluorescence signal is collected at 60°C; After the experiment, the standard curve and dissolution curve were observed, and the experimental results were derived. The expression level of gene RNA was analyzed by 2-ΔΔCt method. The amplification primers of the target genes are shown in Table 2. The experiment was repeated 3 times. GAPDH was used as an internal reference.

Table 2
HIF-1α and GAPDH primer sequences

Primer	Species	Direction	Sequence (5'→3')
HIF-1α	Human	Upstream	5’- GAACGTCGAAAAGAAAAGTCTCG – 3’
		Downstream	5’- CCTTATCAAGATGCGAACTCACA – 3’
GAPDH	Human	Upstream	5’- GGAGCGAGATCCCTCCAAAAT-3’
		Downstream	5’- GGCTGTTGTCATACTTCTCATGG-3’

2.7 CCK-8 detection of cell viability

Follow the instructions of the CCK-8 kit (Servicebio, China). Cells from Control group and HIF-1α group were collected and seeded in 96-well plates at 8×10^3 cells/well, and the time and name of cells per well were marked at the corresponding positions. Each group was provided with 3 repeated holes. The cells were incubated at 37 ℃, 5% CO_2 incubator and 37 ℃ anoxic conditions (92% N_2, 5% CO_2, 3% O_2) according to the requirements of the experiment. After that, CCK-8 kit was used to detect cell viability and proliferation ability. The absorbance of Control, Control + OGD, and shHIF-1α + OGD cells at 450nm at five time points of 0h, 1h, 2h, 3h, and 4h was detected by cell microwell reading instrument (3 wells replicated for each concentration). The mean ± SD is used to represent the results.

2.8 ROS content detection

The detection of reactive oxygen species (ROS) was performed according to the instructions of the kit (Solarbio, China): DCFH-DA was diluted with serum-free medium at a ratio of 1: 1000 to achieve a final concentration of 10 μmol/L. Remove the cell culture medium and add an appropriate volume of diluted DCFH-DA. 1 ml of diluted DCFH-DA was added to one well of the six-well plate. Incubate in a cell incubator at 37°C for 20 min. The cells were washed three times with serum-free cell culture broth to sufficiently remove DCFH-DA that did not enter the cells. Direct observation with a fluorescence microscope.

2.9 Detection of MDA content with kit

The level of lipid oxidation can be detected by detecting the level of MDA. Follow the instructions of Malondialdehyde Detection Kit (Solarbio, China) as follows: Collect cells into centrifuge tubes and discard supernatant after centrifugation; Add 1ml of extract solution per 5 million cells, disrupt the cells by ultrasonic ultrasound, centrifuge at 4 ℃, take the supernatant, and place it on ice for measurement. The mixed solution was kept in a 100°C water bath for 60 minutes, then cooled in an ice bath, 10,000 g,

at room temperature, and centrifuged for 10 minutes. 200 μl of the supernatant was aspirated into a 96-well plate and the absorbance of each sample at 532 nm and 600 nm was measured to calculate the MDA content.

2.10 Western blotting

Total proteins from cells were extracted using RIPA lysis buffer and 1% PMSF added to protease inhibitor cocktail. Protein concentration was measured using the BCA protein assay kit. According to the experimental requirements, 8% PAGE gel was prepared. Equal amounts of sample proteins were loaded onto SDS-PAGE gels, separated by electrophoresis, and then transferred onto PVDF membranes. After sealing with 5% skim milk for 2 hours at room temperature, it was washed 3 times with TBST buffer for 5 minutes. The target protein was incubated with the corresponding primary antibody (Immunoway; America; 1: 1000) overnight at 4°C and then incubated with skim milk containing the secondary antibody (Solarbio; China; 1: 10000) at the concentration described above for 2 h. Immune signals were detected using electrochemiluminescence, ECL using Western Blot Reagent Pack (Bio-Rad, Hercules, Calif.) and Fusion Solo imaging system (Germany). ImageJ analysis software was used to quantify gray values (n = 3).

2.11 Constructing a CeRNA regulatory network related to HIF-1α

The lncRNA-miRNA regulatory relationships were first determined using the DIANA-LncBase (v2) database. thresholds > = 0.715 as the standard. The top 30 lncRNA-miRNA regulatory relationships were selected according to the thresholds value. Secondly, the miRNA-mRNA regulatory relationships were determined using the miRTarBase database, and the top 30 miRNA-mRNA regulatory relationships were selected after sorting from high according to the evidence validity of the validation method. Finally, cytoscape was used to construct an lncRNA-miRNA-mRNA regulatory network.

2.12 Studies on pSICHECK2-lncHIF1A-AS2 and miR-27a-3p regulatory networks with dual luciferase reporter system

The cloning sites of psicheck2-HIF-1α-WT, psicheck2-HIF1A-Mut, psicheck2-HIF-1α-AS2-Mut1 and psicheck2-HIF-1α-AS2-WT were constructed as Xho □, and the corresponding sequences were synthesized by chemical synthesis.

2.13 Statistical analysis

ImageJ software calculated the gray value of Western Blot bands, and analyzed the relative expression of Western Blot experimental protein bands. The experimental data were analyzed and plotted using GraphPad Prism 9.5.1. Data were obtained from at least 3 replicates of all experiments. The independent sample T-test was used to compare the differences between the two groups. One-way ANOVA was used

to analyze differences between groups. Mean ± standard deviation (SD) is shown in this study. The difference was statistically significant with $P < 0.05$.

2.14 Use of AI-assisted tools

ChatGPT (OpenAI) was used to assist with revision of the title, abstract, and discussion and with manuscript formatting. This use did not include generation of experimental data or scientific images.

3. Results

3.1 Differential expression of HIF-1α at mRNA level

The mRNA data of IS-related dataset GSE16561 was downloaded from GEO database, and the expression of HIF-1α in ischemic stroke group and control group was analyzed. The results showed that the expression of HIF-1α was elevated in the ischemic stroke group, see Fig. 1.

3.2 Construction of PPI protein network associated with HIF-1α gene, Gene Ontology (GO) and Kyoto Encyclopedia of Genes and Genomes (KEGG) enrichment analysis

The PPI network associated with the HIF-1α gene was constructed using the STRING online tool, as shown in Fig. 2a. GO and KEGG investigated the related mechanisms of HIF-1α in ischemic stroke. GO analysis found that BP was mainly enriched in response to decreased oxygen levels, in response to hypoxia, and in response to oxygen levels. CC is mainly a transcriptional regulatory complex, a protein acetyltransferase complex, and a histone acetyltransferase complex. MF is mainly DNA-binding transcription factor binding, RNA polymerase II-specific DNA-binding transcription factor binding, p53 binding. KEGG revealed a focus on renal cell carcinoma, HIF-1 signaling pathway, prostate cancer. See Fig. 2b.

3.3 HIF-1α-related regulatory networks

lncHIF1A-AS2 adsorbed onto miR-27a-3p as a molecular sponge to regulate the expression of miR-27a-3p; miR-27a-3p regulates the expression of HIF-1α upon binding to HIF-1α (Fig. 3).

3.4 Infection with silent HIF-1α lentivirus

After shHIF-1α lentivirus infected hCMEC/D3 cells, the total RNA of shHIF-1α group and negative control group were extracted and reverse transcribed into cDNA, RT-qPCR and WB assay were used to detect the expression level of HIF-1α in each group. As shown in Fig. 4a, the expression level of HIF-1α mRNA in the shHIF-1α group was reduced ($P = 0.0036$). And was further verified at the protein level, As shown in Fig. 4b, the protein expression of HIF-1α in the shHIF-1α group decreased, And all the above experiments were statistically significant ($P = 0.0038$). It is suggested that lentiviral infection of hCMEC/D3 is successful.

3.5 HIF-1α knockdown increases CCK-8 signals after OGD

After inoculation, the growth density of cells reached about 50%. At this time point as 0h, the glucose and oxygen deprivation experiment was carried out, and the OGD time was 2h. Microscopic observation and CCK-8 experiment were performed at 0h, 1h, 2h, 3h and 4h, respectively, the results showed that the cell state under the microscope was displayed with 3h as a representative, the cell density was greater in the Control group and lower in the other two groups (Fig. 5a), Cell viability was significantly inhibited at the onset of OGD 2 h, whereas cell viability increased in the shHIF-1α + OGD group (Fig. 5B).

3.6 RT-qPCR and WB test were used to detect the expression of HIF-1α in each group

After shHIF-1α lentivirus infection of hCMEC/D3 cells, the total RNA of hCMEC/D3 cells in Control group, Control + OGD group, shHIF-1α group and shHIF-1α + OGD group were extracted respectively, after reverse transcription into cDNA. RT-qPCR and WB assay were used to detect the mRNA and protein expression levels of HIF-1α in each group, respectively. As shown in Fig. 6, the expression level of HIF-1α is affected by OGD, and the expression level is elevated after OGD.

3.7 Effect of silencing HIF-1α on the expression of ROS and MDA in hCMEC/D3 cells of OGD model

To further evaluate the effect of silencing HIF-1α in hCMEC/D3 cell OGD model, we illustrated by detecting the content of ROS and MDA. The experiment was performed according to the instructions of the kit, and the morphology showed the variation of ROS between different groups (Fig. 7a). The expression levels of ROS in different experimental groups were detected. It was found that the content of ROS in shHIF-1α + OGD group was higher than that in shHIF-1α group, and the content of ROS in Control + OGD group was also higher than that in Control group (Fig. 7b). Compared with the Control group, the MDA content in the Control + OGD group cells was elevated, and the shHIF-1α + OGD group MDA content was also elevated relative to the Control + OGD group. This suggests that OGD elevates lipid oxidation levels of cells (Fig. 7C).

3.8 Dual luciferase experiments predict the interaction between pSICHECK2-lncHIF1A-AS2 and miR-27a-3p

Dual luciferase assay was used to detect and analyze the interaction between pSICHECK2-lncHIF1A-AS2-WT1/2 and miR-27a-3p. The experimental results showed that after co-transfection of pSICHECK2-lncHIF1A-AS2-WT1/2 and miR-27a-3p mimics, the luciferase activity was significantly reduced, as shown in Fig. 8a. After co-transfection of pSICHECK2-HIF-1α-WT with miR-27a-3p mimics (mimics), luciferase activity was significantly reduced, see Fig. 8b.

4. Discussion

Hypoxia caused by impaired cerebral blood flow contributes to metabolic dysfunction and cellular injury during ischemic stroke. In this study, HIF-1α knockdown was associated with increased CCK-8 signals in OGD-treated hCMEC/D3 cells, but this change was accompanied by higher MDA levels than in the Control + OGD group. These findings reveal divergent responses of the CCK-8 readout and the lipid peroxidation marker and do not support a uniform antioxidant or cytoprotective effect of HIF-1α knockdown. The bioinformatic and reporter analyses additionally suggest a putative HIF1A-AS2/miR-27a-3p/HIF1A regulatory relationship, although its causal contribution to these cellular responses remains unestablished.

Hypoxia-inducible factor 1 (HIF1) is a transcription factor that plays an important regulatory role in oxygen homeostasis by controlling the transfer and utilization of oxygen [19]. Bioinformatics studies have found that the expression of HIF-1α in IS is differential and highly expressed in IS patients. It plays a wide range of roles in the pathophysiology of stroke by regulating multiple pathways, including glucose metabolism, angiogenesis, neuronal survival, neuroinflammation, and blood-brain barrier regulation [20]. At normal oxygen levels, most of the molecular oxygen delivered to the cell is used to produce adenosine triphosphate (ATP) through mitochondrial oxidative phosphorylation, thereby meeting cellular metabolic needs. Thereafter, prolyl hydroxylase (PHD) promotes HIF degradation, resulting in inhibition of HIF transcriptional activity, thus reducing the expression of HIF-1α mRNA and protein. In hypoxia, almost all oxygen molecules are used by mitochondria, resulting in the inhibition of hydroxylase. Stable HIF-1α forms a dimer with HIF-1β, resulting in increased transcriptional expression of HIF-dependent genes and thus HIF-1α mRNA and protein [21]. The expression of HIF-1α mRNA in the spatial and temporal regions was induced at 7.5h after ischemia in the infarcted brain and further increased at 19 and 24h after ischemia [20]. Another study reported that in a mouse model of permanent middle cerebral artery occlusion (pMCAO) model, HIF-1α mRNA in the periinfarct region peaked at 24h after ischemia [22]. At the cellular level, we studied that hCMEC/D3 cells treated with OGD for 2h, and the expression level of HIF-1α was elevated. Rodent studies have shown that regulation of HIF-1α expression has a good effect in the treatment of ischemic stroke, but the intrinsic regulation of HIF-1α expression in vivo is a complex process [23]. After HIF-1α knockdown, CCK-8 signals increased under OGD. Because this assay reflects cellular metabolic activity, the increase alone cannot establish enhanced proliferation or an overall protective effect, particularly in the presence of higher MDA levels. In the OGD study of cultured cardiomyocytes in vitro, the content of HIF-1α in the supernatant of cultured cardiomyocytes increased after oxygen deprivation [24]; Moreover, in endothelial cells, HIF-1α protein expression increased during acute hypoxia [25].

Some conclusive evidence suggests that low blood flow during IS triggers some reactions that produce free radicals (marked by elevated MDA) and damage DNA [26]. Malondialdehyde (MDA) and 4-hydroxynonenal (4-HNE) are the most commonly used biomarkers of oxidative stress, i.e. lipid peroxidation [27]. MDA is a key marker of cell membrane oxidation and represents a mechanism of brain damage that occurs throughout ischemic stroke cascade [28]. In the present study, MDA levels were higher in the shHIF-1α + OGD group than in the Control + OGD group, as reported in Section 3.7 and shown in Fig. 7c. Thus, the MDA findings do not support attenuation of lipid peroxidation by HIF-1α

knockdown under the tested OGD conditions. The coexistence of increased CCK-8 signals and higher MDA indicates that the two endpoints did not change in a uniformly protective direction. A possible explanation is that changes in cellular metabolic activity do not necessarily track changes in lipid peroxidation; however, this explanation was not directly tested. Independent measurements of cell number, cell death, and lipid peroxidation are needed to clarify the biological significance of these divergent responses.

It has been reported in the literature that IS leads to oxidative stress through the production of excessive reactive oxygen species and other substances, which is a complication of cerebral ischemia-reperfusion injury (IRI) and can activate matrix metalloproteinases, leading to the degradation of extracellular matrix and altered BBB permeability [29]. The main reason is the imbalance between the excessive production of ROS and the intrinsic antioxidant capacity, which leads to pathological progression of ischemic brain injury and causes oxidative damage [26]. ROS usually promotes acute brain damage after stroke has been a leading cause of death worldwide [30, 31]. A growing body of studies has highlighted the close link between excess ROS production and stroke-induced inflammatory responses [32]. Ischemic stroke generates an immune response that leads to neuronal loss and tissue repair, a complex process that involves a range of cell types and effector molecules and affects tissues outside the central nervous system [33]. Inflammation plays an important role in the exacerbation of ischemic stroke and other diseases, and its targeted therapy is considered to be an effective method to reduce injury [34–36]. Appropriate termination of cell death-induced neuroinflammation is a prerequisite for tissue repair in AIS [37]. Previous studies have found that HIF-1α gene is closely related to ROS production and oxidative stress. Ischemia and reperfusion induce a large number of ROS production, which is the core pathological cause of irreversible damage to the infarct core and surrounding viable penumbra in ischemic hemisphere [38, 39]. ROS is a unifying mechanism of many pathophysiological processes, capable of destroying DNA and causing peroxidation of unsaturated fatty acids in the cell membrane, thus changing the integrity of cells [40]. Silencing HIF-1α may alleviate inflammation and oxidative stress in IS via the CXCR4/NF-κB pathway [41]. In the present cell experiments, OGD increased ROS levels relative to the corresponding non-OGD conditions in both control and HIF-1α-knockdown cells. ROS was not measured in patient samples in this study. The reported comparisons do not establish a consistent reduction in OGD-associated oxidative stress following HIF-1α knockdown, and the increase in MDA further argues against a general antioxidant interpretation. Differences from earlier studies should therefore be considered in relation to the experimental model, exposure conditions, and measured endpoints, without assuming a common protective mechanism.

The ceRNA hypothesis reveals a novel mechanism of RNA interaction, representing a novel gene expression regulation mode, and the regulatory network is more elaborate and complex, involving multiple types of RNA molecules, including mRNA, pseudogene transcripts, lncRNA, and circRNA [42, 43]. miRNAs are small non-coding RNA molecules that regulate gene expression by affecting mRNA stability or translation efficiency [44]. Involved in multiple mechanisms of stroke pathophysiology and recovery including apoptosis, inflammation, angiogenesis, oxidative stress, ischemia, and blood-brain

barrier dysfunction [45]. lncRNA and circRNA can act as competitive endogenous RNA (ceRNA), attenuating the inhibition of targeted messenger RNA (mRNA) by microRNA (miRNA) [46] .

In the study of ischemic cerebral infarction, it was found that lncHIF1A-AS2 must bind to miRNA before it can regulate HIF-1α expression [47]; In cultured HUVECs cells, lncHIF1A-AS2 binds to miR-153-3p as a molecular sponge to regulate HIF-1α expression [48]; Inhibition of lncHIF1A-AS2 can protect against damage due to atherosclerosis [12] ; Knockdown of lncHIF1A-AS2 can protect cardiac injury caused by ischemia and hypoxia [24]; lncHIF1A-AS2 has the function of regulating target gene expression after binding to miRNA [48]. Previous studies have found that five miRNAs, including miR-27a-3p, can be used as molecular markers for diagnosis of ischemic cerebral infarction and molecular targets for treatment of ischemic cerebral infarction [49]. In addition, in the OGD model of cultured H9C2 cells, it was found that lncRNA-BNIP3 binds to miR-27a-3p in the form of molecular sponge, and regulates the expression of target genes to mediate hypoxia-induced injury [50]; It is consistent with the results of dual luciferase experiment.

This study has several limitations. First, the functional experiments were performed in a single endothelial cell line without in vivo validation. Second, CCK-8 measurements alone cannot distinguish changes in cell number from changes in cellular metabolic activity and are insufficient to establish enhanced proliferation. Third, the divergent CCK-8 and MDA responses preclude a definitive conclusion that HIF-1α knockdown protects against OGD-induced injury. Additional cell-death assays and independent lipid peroxidation measurements are required. Finally, the reporter assays do not establish that an endogenous HIF1A-AS2/miR-27a-3p/HIF1A axis mediates these effects; coordinated expression analyses and functional rescue experiments are needed to test this proposed mechanism.

5. Conclusion

HIF-1α knockdown was associated with increased CCK-8 signals but higher MDA levels in OGD-treated hCMEC/D3 cells. The findings therefore indicate divergent effects on the metabolic viability readout and lipid peroxidation, rather than a demonstrated reduction in oxidative injury. The reporter assays support putative interactions involving HIF1A-AS2, miR-27a-3p, and HIF1A, but their role in the observed phenotype remains to be established. These results support further investigation of the context-dependent effects of HIF-1α in brain endothelial responses to oxygen–glucose deprivation.

Declarations

Competing interests

All authors declare no competing interests.

Ethics approval and consent to participate

Not applicable.

Consent for publication

Not applicable.

Funding

This study was supported by the National Natural Science Foundation of China (grant no. 82160244). Nantong City Research Project (grant no.QN2025075).

Author Contribution

Min Wang designed the methodology, conducted the investigation, performed formal analyses of the raw data, curated the data, provided insights or reagents, and wrote the original draft. All authors analyzed the processed data. Guangming Wang and Huaqiu Chen reviewed and edited the manuscript and supervised the project. All authors read and approved the final manuscript.

Data availability

The public transcriptomic datasets listed in Table 1 are available from the Gene Expression Omnibus (https://www.ncbi.nlm.nih.gov/geo/) under accession numbers GSE16561, GSE58294, GSE22255, GSE37587, GSE25414, and GSE119121.

References

1. Feigin VL, Brainin M, Norrving B, Martins SO, Pandian J, Lindsay P et al (2025) World Stroke Organization: Global Stroke Fact Sheet 2025. Int J Stroke 20:132–144. https://doi.org/10.1177/17474930241308142
2. Strilciuc S, Grad DA, Radu C, Chira D, Stan A, Ungureanu M et al (2021) The economic burden of stroke: a systematic review of cost of illness studies. J Med Life 14:606–619. https://doi.org/10.25122/jml-2021-0361
3. Tuo QZ, Zhang ST, Lei P (2022) Mechanisms of neuronal cell death in ischemic stroke and their therapeutic implications. Med Res Rev 42:259–305. https://doi.org/10.1002/med.21817
4. Sato T, Takeda N (2023) The roles of HIF-1α signaling in cardiovascular diseases. J Cardiol 81:202–208. https://doi.org/10.1016/j.jjcc.2022.09.002
5. Yao H, Tian J, Cheng S, Dou H, Zhu Y (2024) The mechanism of hypoxia-inducible factor-1α enhancing the transcriptional activity of transferrin ferroportin 1 and regulating the Nrf2/HO-1

pathway in ferroptosis after cerebral ischemic injury. Neuroscience 559:26–38. https://doi.org/10.1016/j.neuroscience.2024.08.025

6. Xue Z, Li H, Xie W, Xu Y, Zhou L, Qu ZB (2022) Benzo[d]isoxazole Derivatives as Hypoxia-Inducible Factor (HIF)-1α Inhibitors. ACS Med Chem Lett 13:1864–1869. https://doi.org/10.1021/acsmedchemlett.2c00308
7. Chen H, Ma D, Yue F, Qi Y, Dou M, Cui L et al (2022) The Potential Role of Hypoxia-Inducible Factor-1 in the Progression and Therapy of Central Nervous System Diseases. Curr Neuropharmacol 20:1651–1666. https://doi.org/10.2174/1570159x19666210729123137
8. Jiang S, Guo C, Zhang W, Che W, Zhang J, Zhuang S et al (2019) The Integrative Regulatory Network of circRNA, microRNA, and mRNA in Atrial Fibrillation. Front Genet 10:526. https://doi.org/10.3389/fgene.2019.00526
9. Ewida HA, Zayed RK, Darwish HA, Shaheen AA (2021) Circulating lncRNAs HIF1A-AS2 and LINLK-A: Role and Relation to Hypoxia-Inducible Factor-1α in Cerebral Stroke Patients. Mol Neurobiol 58:4564–4574. https://doi.org/10.1007/s12035-021-02440-8
10. Tuluhong D, Dunzhu W, Wang J, Chen T, Li H, Li Q et al (2020) Prognostic Value of Differentially Expressed LncRNAs in Triple-Negative Breast Cancer: A Systematic Review and Meta-Analysis. Crit Rev Eukaryot Gene Expr 30:447–456. https://doi.org/10.1615/CritRevEukaryotGeneExpr.2020035836
11. Liu J, Zhao G, Liu XL, Zhang G, Zhao SQ, Zhang SL et al (2021) Progress of non-coding RNAs in triple-negative breast cancer. Life Sci 272:119238. https://doi.org/10.1016/j.lfs.2021.119238
12. Li P, Xing J, Zhang J, Jiang J, Liu X, Zhao D et al (2020) Inhibition of long noncoding RNA HIF1A-AS2 confers protection against atherosclerosis via ATF2 downregulation. J Adv Res 26:123–135. https://doi.org/10.1016/j.jare.2020.07.015
13. Li X, Xu M, Ding L, Tang J (2019) MiR-27a: A Novel Biomarker and Potential Therapeutic Target in Tumors. J Cancer 10:2836–2848. https://doi.org/10.7150/jca.31361
14. Yasmeen S, Kaur S, Mirza AH, Brodin B, Pociot F, Kruuse C (2019) miRNA-27a-3p and miRNA-222-3p as Novel Modulators of Phosphodiesterase 3a (PDE3A) in Cerebral Microvascular Endothelial Cells. Mol Neurobiol 56:5304–5314. https://doi.org/10.1007/s12035-018-1446-5
15. Yang K, Zeng L, Ge A, Wang S, Zeng J, Yuan X et al (2022) A systematic review of the research progress of non-coding RNA in neuroinflammation and immune regulation in cerebral infarction/ischemia-reperfusion injury. Front Immunol 13:930171. https://doi.org/10.3389/fimmu.2022.930171
16. Neag MA, Mitre AO, Burlacu CC, Inceu AI, Mihu C, Melincovici CS et al (2022) miRNA Involvement in Cerebral Ischemia-Reperfusion Injury. Front Neurosci 16:901360. https://doi.org/10.3389/fnins.2022.901360
17. Yang R, Xu B, Yang B, Fu J, Chen H, Wang X (2021) Non-coding RNAs: the extensive and interactive regulators of the blood-brain barrier permeability. RNA Biol 18:108–116. https://doi.org/10.1080/15476286.2021.1950465

18. Sun P, Hamblin MH, Yin KJ (2022) Non-coding RNAs in the regulation of blood-brain barrier functions in central nervous system disorders. Fluids Barriers CNS 19:27. https://doi.org/10.1186/s12987-022-00317-z
19. Semenza GL (2014) Hypoxia-inducible factor 1 and cardiovascular disease. Annu Rev Physiol 76:39–56. https://doi.org/10.1146/annurev-physiol-021113-170322
20. Vatte S, Ugale R (2023) HIF-1, an important regulator in potential new therapeutic approaches to ischemic stroke. Neurochem Int 170:105605. https://doi.org/10.1016/j.neuint.2023.105605
21. Malkov MI, Lee CT, Taylor CT (2021) Regulation of the Hypoxia-Inducible Factor (HIF) by Pro-Inflammatory Cytokines. Cells 10:2340. https://doi.org/10.3390/cells10092340
22. Marti HJ, Bernaudin M, Bellail A, Schoch H, Euler M, Petit E et al (2000) Hypoxia-induced vascular endothelial growth factor expression precedes neovascularization after cerebral ischemia. Am J Pathol 156:965–976. https://doi.org/10.1016/s0002-9440(10)64964-4
23. Camps C, Saini HK, Mole DR, Choudhry H, Reczko M, Guerra-Assunção JA et al (2014) Integrated analysis of microRNA and mRNA expression and association with HIF binding reveals the complexity of microRNA expression regulation under hypoxia. Mol Cancer 13:28. https://doi.org/10.1186/1476-4598-13-28
24. Luo F, Wu Y, Zhu L, Zhang J, Liu Y, Jia W (2020) Knockdown of HIF1A-AS2 suppresses TRIM44 to protect cardiomyocytes against hypoxia-induced injury. Cell Biol Int 44:1523–1534. https://doi.org/10.1002/cbin.11348
25. Chamboredon S, Ciais D, Desroches-Castan A, Savi P, Bono F, Feige JJ et al (2011) Hypoxia-inducible factor-1α mRNA: a new target for destabilization by tristetraprolin in endothelial cells. Mol Biol Cell 22:3366–3378. https://doi.org/10.1091/mbc.E10-07-0617
26. Su XT, Wang L, Ma SM, Cao Y, Yang NN, Lin LL et al (2020) Mechanisms of Acupuncture in the Regulation of Oxidative Stress in Treating Ischemic Stroke. Oxid Med Cell Longev 2020:7875396. https://doi.org/10.1155/2020/7875396
27. Tsikas D (2017) Assessment of lipid peroxidation by measuring malondialdehyde (MDA) and relatives in biological samples: Analytical and biological challenges. Anal Biochem 524:13–30. https://doi.org/10.1016/j.ab.2016.10.021
28. Zhang L, Li D, Zhang C, Zhang J, Xu J, Bai L et al (2024) Predictive value of serum MDA and 4-HNE levels on the occurrence of early neurological deterioration after intravenous thrombolysis with rt-PA IVT in patients with acute ischemic stroke. J Stroke Cerebrovasc Dis 33:107574. https://doi.org/10.1016/j.jstrokecerebrovasdis.2024.107574
29. Gholamzadeh R, Ramezani F, Tehrani PM, Aboutaleb N (2021) Apelin-13 attenuates injury following ischemic stroke by targeting matrix metalloproteinases (MMP), endothelin- B receptor, occludin/claudin-5 and oxidative stress. J Chem Neuroanat 118:102015. https://doi.org/10.1016/j.jchemneu.2021.102015
30. Yingze Y, Zhihong J, Tong J, Yina L, Zhi Z, Xu Z et al (2022) NOX2-mediated reactive oxygen species are double-edged swords in focal cerebral ischemia in mice. J Neuroinflammation 19:184.

https://doi.org/10.1186/s12974-022-02551-6

31. Yang Y, Li Z, Fan X, Jiang C, Wang J, Rastegar-Kashkooli Y et al (2024) Nanozymes: Potential Therapies for Reactive Oxygen Species Overproduction and Inflammation in Ischemic Stroke and Traumatic Brain Injury. ACS Nano 18:16450–16467. https://doi.org/10.1021/acsnano.4c03425
32. Candelario-Jalil E, Dijkhuizen RM, Magnus T (2022) Neuroinflammation, Stroke, Blood-Brain Barrier Dysfunction, and Imaging Modalities. Stroke 53:1473–1486. https://doi.org/10.1161/strokeaha.122.036946
33. DeLong JH, Ohashi SN, O'Connor KC, Sansing LH (2022) Inflammatory Responses After Ischemic Stroke. Semin Immunopathol 44:625–648. https://doi.org/10.1007/s00281-022-00943-7
34. Amani H, Shahbazi MA, D'Amico C, Fontana F, Abbaszadeh S, Santos HA (2021) Microneedles for painless transdermal immunotherapeutic applications. J Control Release 330:185–217. https://doi.org/10.1016/j.jconrel.2020.12.019
35. Cai Y, Leng S, Ma Y, Xu T, Chang D, Ju S (2021) Dynamic change of MMP-9 in diabetic stroke visualized by optical imaging and treated with CD28 superagonist. Biomater Sci 9:2562–2570. https://doi.org/10.1039/d0bm02014a
36. Kelly PJ, Lemmens R, Tsivgoulis G (2021) Inflammation and Stroke Risk: A New Target for Prevention. Stroke 52:2697–2706. https://doi.org/10.1161/strokeaha.121.034388
37. Cai W, Hu M, Li C, Wu R, Lu D, Xie C et al (2023) FOXP3 + macrophage represses acute ischemic stroke-induced neural inflammation. Autophagy 19:1144–1163. https://doi.org/10.1080/15548627.2022.2116833
38. Ye H, Ma Z, Liu L, Zhang T, Han Q, Xiang Z et al (2022) Thrombus Inhibition and Neuroprotection for Ischemic Stroke Treatment through Platelet Regulation and ROS Scavenging. ChemMedChem 17:e202200317. https://doi.org/10.1002/cmdc.202200317
39. Qin C, Yang S, Chu YH, Zhang H, Pang XW, Chen L et al (2022) Signaling pathways involved in ischemic stroke: molecular mechanisms and therapeutic interventions. Signal Transduct Target Ther 7:215. https://doi.org/10.1038/s41392-022-01064-1
40. Orellana-Urzúa S, Rojas I, Líbano L, Rodrigo R (2020) Pathophysiology of Ischemic Stroke: Role of Oxidative Stress. Curr Pharm Des 26:4246–4260. https://doi.org/10.2174/1381612826666200708133912
41. Chen G, Wang X, Jin Z, Hu GB, Yu QH, Jiang HY (2024) HIF-1α knockdown attenuates inflammation and oxidative stress in ischemic stroke male rats via CXCR4/NF-κB pathway. Brain Behav 14:e70039. https://doi.org/10.1002/brb3.70039
42. Wang Y, Zhou G, Guan T, Wang Y, Xuan C, Ding T et al (2022) A network-based matrix factorization framework for ceRNA co-modules recognition of cancer genomic data. Brief Bioinform 23:bbac154. https://doi.org/10.1093/bib/bbac154
43. Lin W, Liu H, Tang Y, Wei Y, Wei W, Zhang L et al (2021) The development and controversy of competitive endogenous RNA hypothesis in non-coding genes. Mol Cell Biochem 476:109–123. https://doi.org/10.1007/s11010-020-03889-2

44. Vishnoi A, Rani S (2023) miRNA Biogenesis and Regulation of Diseases: An Updated Overview. Methods Mol Biol 2595:1–12. https://doi.org/10.1007/978-1-0716-2823-2_1
45. Pir GJ, Zahid MA, Akhtar N, Ayadathil R, Pananchikkal SV, Joseph S et al (2024) Differentially expressed miRNA profiles of serum derived extracellular vesicles from patients with acute ischemic stroke. Brain Res 1845:149171. https://doi.org/10.1016/j.brainres.2024.149171
46. Sufianova G, Shumadalova A, Wenhao Y, Gareev I (2022) Long non-coding RNAs as biomarkers and therapeutic targets for ischemic stroke. Noncoding RNA Res 7:226–232. https://doi.org/10.1016/j.ncrna.2022.09.004
47. Dong P, Li Q, Han H (2022) HIF–1α in cerebral ischemia (Review). Mol Med Rep 25:41. https://doi.org/10.3892/mmr.2021.12557
48. Li L, Wang M, Mei Z, Cao W, Yang Y, Wang Y et al (2017) lncRNAs HIF1A-AS2 facilitates the up-regulation of HIF-1α by sponging to miR-153-3p, whereby promoting angiogenesis in HUVECs in hypoxia. Biomed Pharmacother 96:165–172. https://doi.org/10.1016/j.biopha.2017.09.113
49. Yang X, Wang P, Yan S, Wang G (2022) Study on potential differentially expressed genes in stroke by bioinformatics analysis. Neurol Sci 43:1155–1166. https://doi.org/10.1007/s10072-021-05470-1
50. Li Y, Ren S, Xia J, Wei Y, Xi Y (2020) EIF4A3-Induced circ-BNIP3 Aggravated Hypoxia-Induced Injury of H9c2 Cells by Targeting miR-27a-3p/BNIP3. Mol Ther Nucleic Acids 19:533–545. https://doi.org/10.1016/j.omtn.2019.11.017

Figures

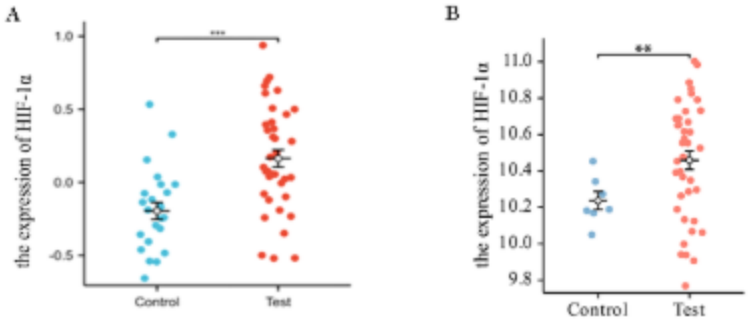


Figure 1

Differential expression of HIF-1α in ischemic stroke group and control group in GEO database (a) Homo sapiens (b) Rattus norvegicus *** P < 0.001, ** P < 0.01

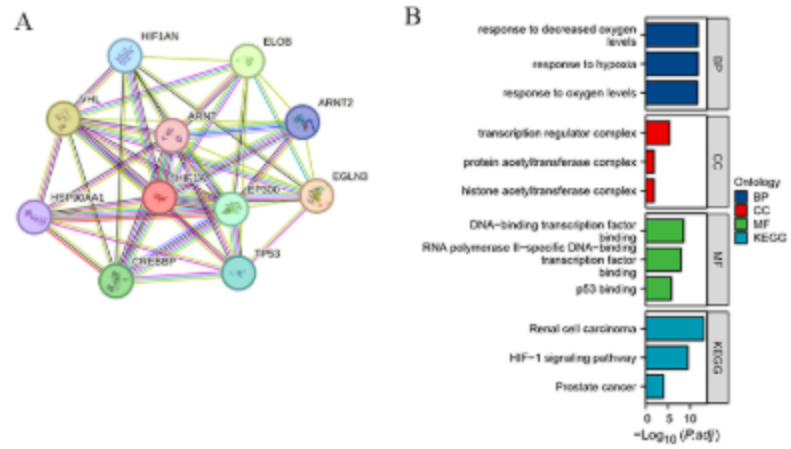


Figure 2

(a) PPI protein interaction network diagram related to the target gene HIF-1α; (b) GO and KEGG enrichment analysis for further analysis of proteins associated with the HIF-1α gene. BP: Biological processes. CC: Cellular component. MF: molecular function

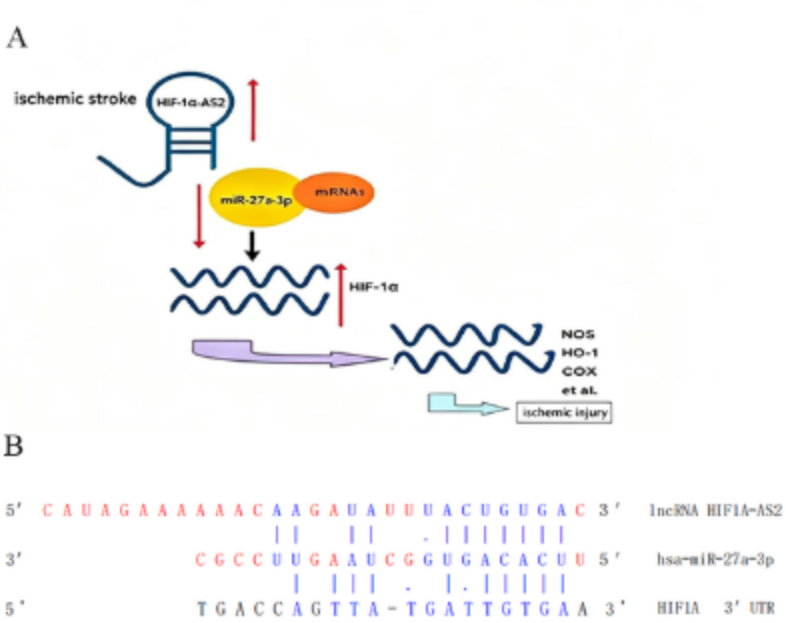


Figure 3

Mechanism of miR-27a-3p/HIF-1α pathway mediated by lncHIF1A-AS2 in ischemic cerebral infarction. (a) Role of the lncHIF1A-AS2/miR-27a-3p/HIF-1α pathway in ischemic stroke; (b) Mechanism of the interaction between lncHIF1A-AS2, miR-27a-3p, HIF-1α

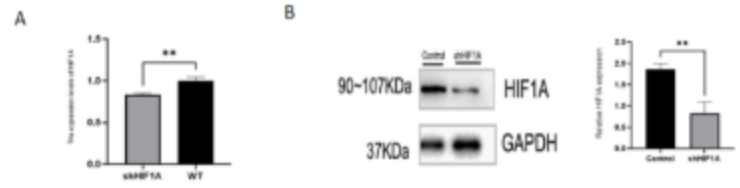


Figure 4

Expression of HIF-1α in hCMEC/D3 cells in two groups. (a) RT-qPCR detection of the mRNA expression level of HIF-1α in the Control and shHIF1-α groups; (b) Western Blot assay was used to detect the expression level of HIF-1α protein in Control group and shHIF1-α group

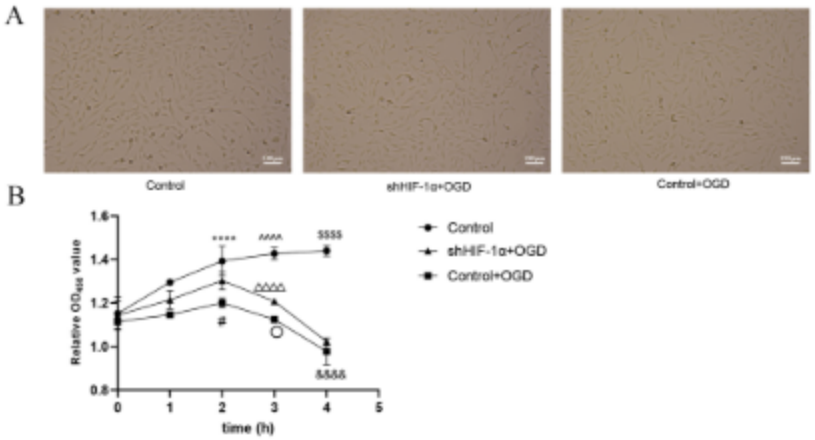


Figure 5

Effect of HIF-1α knockdown on cell morphology and CCK-8 signals. (a) Observation under 3h light microscope. (b) CCK-8 analysis of hCMEC/D3 cells in different experimental groups****P<0.0001,vs. Control+ OGD; #P=0.0119, vs. shHIF-1α+ OGD; ^^^^P<0.0001,vs. Control+ OGD; △△△△P<0.0001,vs. shHIF-1α+ OGD; ○P=0.0439,vs. shHIF-1α+ OGD;

P<0.0001,vs. Control+ OGD; &&&&P<0.0001,vs. shHIF-1α+ OGD

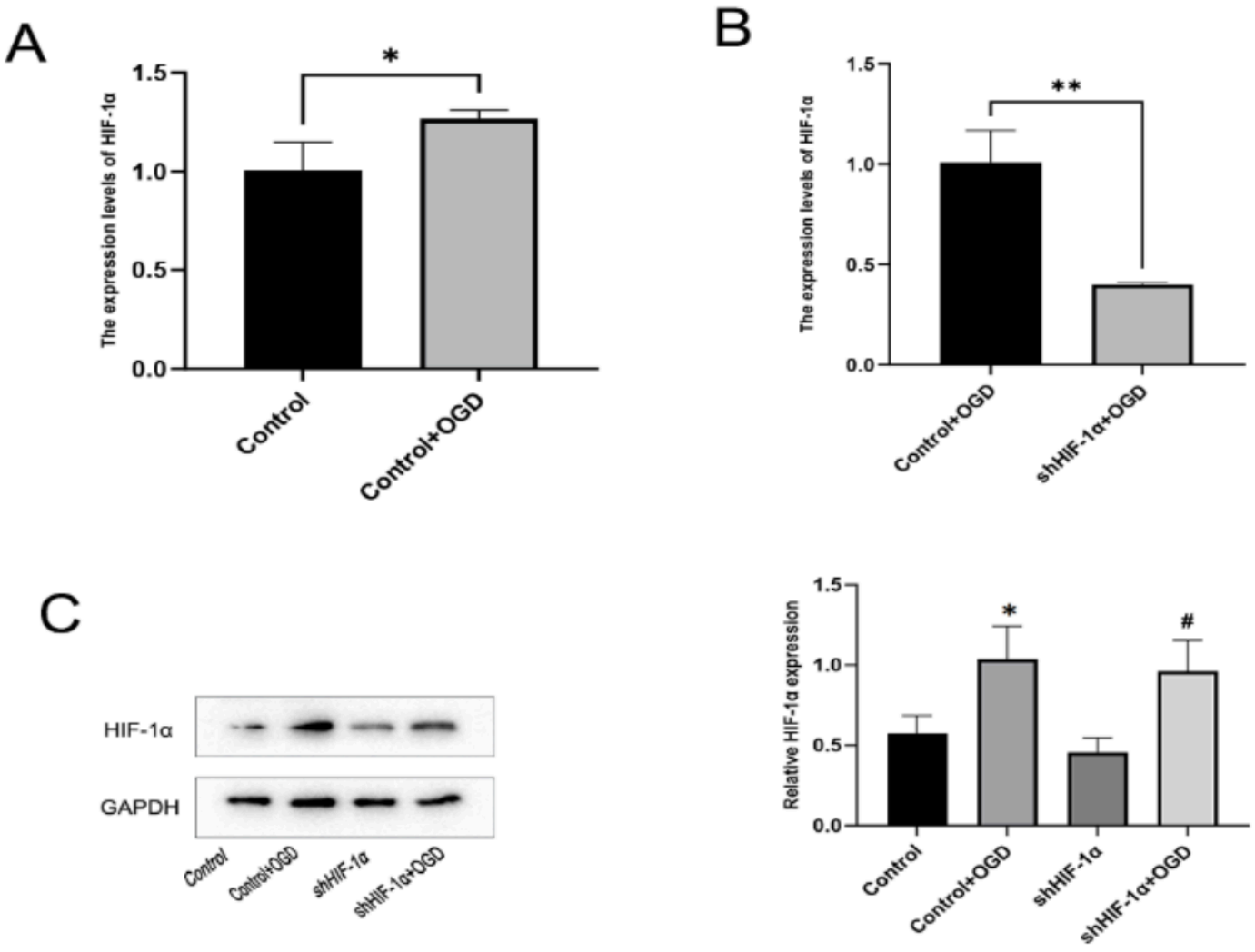


Figure 6

Expression of HIF-1α in different experimental groups. (a) RT-qPCR was used to detect the expression level of HIF-1α mRNA in hCMEC/D3 cells in the Control group and the Control + OGD group; (b) RT-qPCR was used to detect the expression level of HIF-1α mRNA in hCMEC/D3 cells in the Control + OGD group and the shHIF-1α group; (c) Quantitative analysis of HIF-1α after OGD in different experimental groups was detected by Western Blot experiment. *P=0.0275, vs. Control, #P=0.0152, vs. shHIF-1α

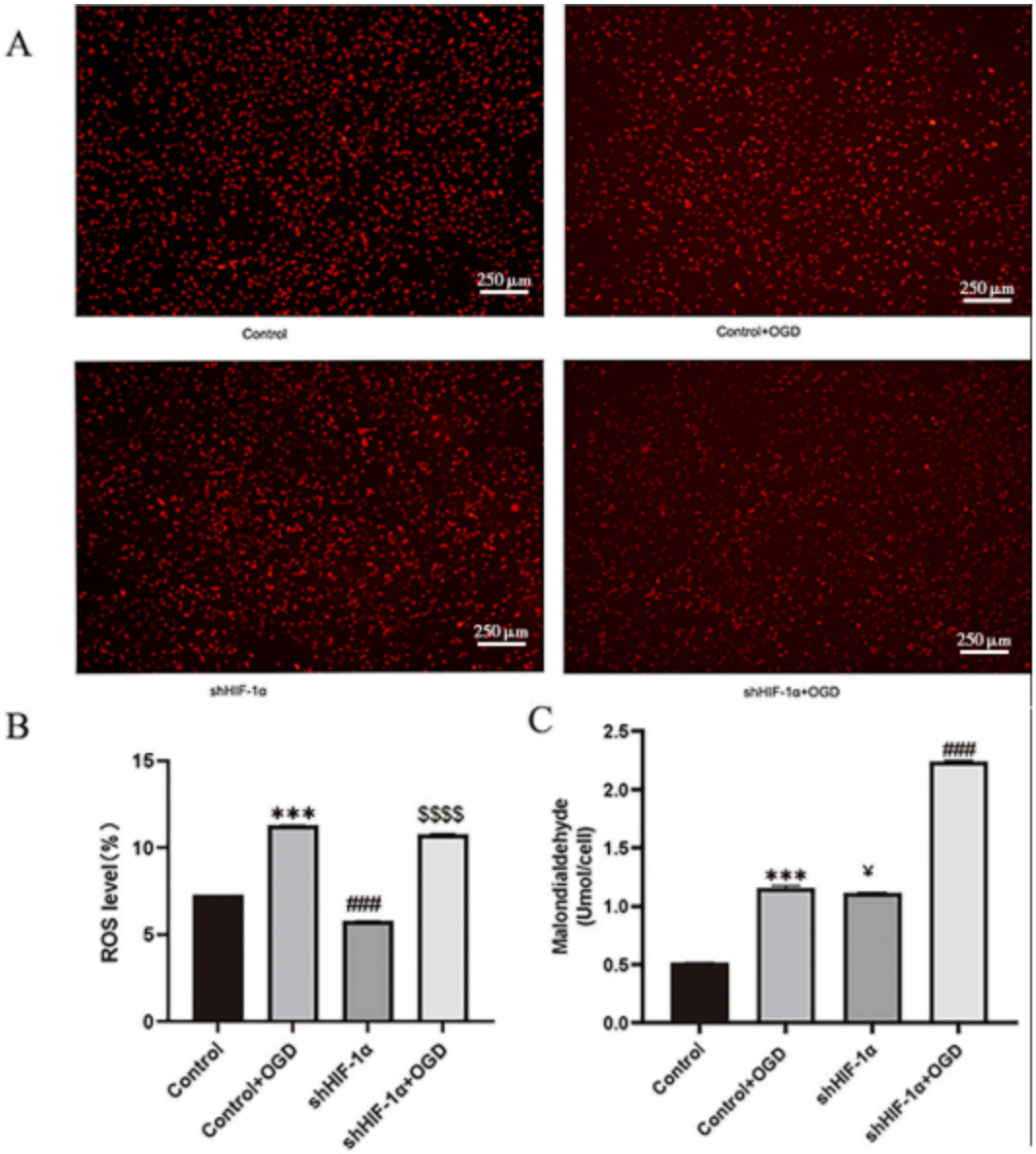


Figure 7

The content of reactive oxygen species (ROS) and malondialdehyde (MDA) in different experimental groups. (a) Morphology shows the changes of ROS among different groups (b) Analyze the content of ROS according to the instructions of the kit for the results of Fig. 7a; (c) Content of MDA between different groups.***P<0.001, vs.Control; ###P<0.001, vs. Control+OGD;

P<0.0001,vs. shHIF-1α

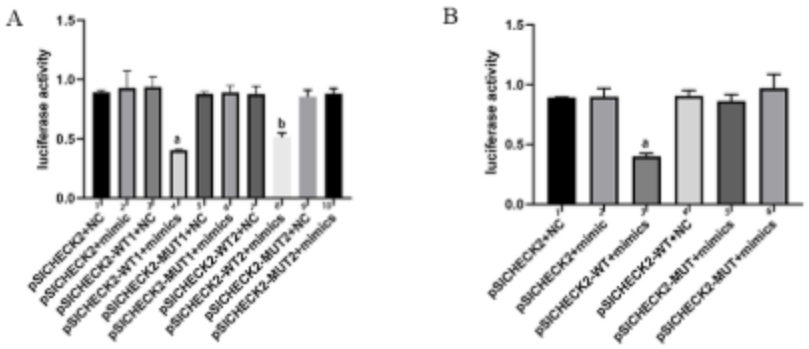


Figure 8

Histogram of dual luciferase system detection. (a) Luciferase activity was significantly reduced after co-transfection of pSICHECK2-lncHIF1A-AS2-WT1/2 with miR-27a-3p mimics (mimics). a represents comparison with 1, 2, 3, 5, 6, 7, 9, 10, $p < 0.0001$, significant difference. b represents comparison with 1, 2, 3, 5, 6, 7, 9, 10, $p < 0.0001$, significant difference; (b) Luciferase activity was significantly reduced after co-transfection of pSICHECK2-HIF-1α-WT with miR-27a-3p mimics (mimics). A represents comparison with 1, 2, 4, 5, 6, $p < 0.0001$, significant difference